Express Polymer Letters Vol.17, No.10 (2023) 1019–1030
Available online at www.expresspolymlett.com
https://doi.org/10.3144/expresspolymlett.2023.76

Research article

Introducing metal-ligand coordination interaction for self-healing and recyclable nitrile–butadiene rubber: A facile strategy

Yuan Gao[1], *Weiran Zhang*[1], *Junhao Wang*[2], *Zishuo Wang*[1], *Zhaobo Wang*[1*]

[1]College of Material Science & Engineering, Qingdao University of Science & Technology, 266042 Qingdao, P. R. China
[2]School of Mechanical, Electrical & Information Engineering, SHANDONG UNIVERSITY, WEIHAI, 264209 Weihai, P. R. China

Received 21 April 2023; accepted in revised form 1 July 2023

Abstract. In this research, a nitrile-butadiene rubber (NBR) was prepared with excellent mechanical, self-healing and recycling properties by introducing metal-ligand coordination interaction. A coordination crosslinking network based on ligand bonding was successfully introduced in the NBR matrix by mechanical compounding. The dynamic reversibility of the coordination crosslinking network not only provides the vulcanizate with excellent mechanical properties but also confers a remarkable self-healing ability under high temperatures and recyclable property under mechanical shear, respectively. The sample, which was subjected to the complete cut, could be capable of restoring its original tensile strength after self-healing treatment. The self-healing efficiency of NBR vulcanizate is significantly dependent on the self-healing temperature and time, which can surprisingly reach 97% of the original tensile strength after self-healing treatment at 180 °C for 60 min. After the mechanical shear, the coordination crosslinking network is reversibly transformed. The tensile strength of the NBR vulcanizates after mechanical shearing recycling and re-vulcanization was similar to that of the original NBR vulcanizates. This research presents a novel approach to enhance the durability of rubber used in commercial applications, endowing it with reshaping and recycling capabilities and mitigating environmental issues associated with waste rubber.

Keywords: *self-healing, coordination, rubber, recycling, mechanical properties*

1. Introduction

Self-healing is one of the most intriguing phenomena in nature. Most organisms could self-heal themselves when they suffer damage. Since White *et al*. [1] first reported the self-healing polymers in 2001, many scholars have attempted to introduce this brilliant and biological concept into synthetic materials. In the last decade, a series of self-healing polymers have been emerged [2–4], which can repair their own damage spontaneously in response to light, heat, or other stimuli. Usually, self-healing polymers can be classified into two distinct categories: extrinsic and intrinsic self-healing materials. Due to the simpler preparation process and the ability to achieve repeated healing, intrinsic self-healing materials are more desirable to researchers. A common approach for constructing intrinsic self-healing materials is to introduce reversible bonds, such as Diels-Alder bonds [5, 6], disulfide bonds [7], hydrogen bonds [8], ionic interactions [3, 9] and metal-ligand coordination [10, 11], *etc*. These dynamic reversible bonds make it feasible to self-heal the broken bonds. Moreover, polymers based on reversible bonds have better chain mobility since the reversible bonds are less restrictive to the polymer crosslinking network, which is also essential for self-healing [9].

*Corresponding author, e-mail: wangzhb@qust.edu.cn

Rubber, as a superior polymer material with a history of application, can be traced back to a century ago. With its unique high elasticity and remarkable mechanical properties, rubber has an irreplaceable wide range of applications in medical materials [12], aerospace [13], automotive industry [14] and other fields. However, during the service, rubber is prone to cracking under stress, light, and heat, resulting in a gradual loss of mechanical properties [15, 16]. In order to improve the strength and rebounded resilience of rubber products, crosslinking is necessary. Unfortunately, the vulcanizates, crosslinked in the traditional way, are difficult to recycle, which could cause serious pollution [17]. However, these methods are complex and ineffective, while the deterioration in the mechanical properties of the recycled product is inevitable [18, 19]. Self-healing materials are a promising solution to improve material sustainability and prolong the lifetime [20, 21]. By constructing the reversible supramolecular networks, rubber is expected to exhibit self-healing and recyclable properties. Nevertheless, rubbers based on reversible supramolecular crosslinking networks often have weak mechanical properties due to relatively weak non-covalent interactions [4]. In order to address this challenge, Liu *et al*. [22] achieved high strength and stability by constructing the ionic-covalent crosslinking networks while failing to consider the mechanical and self-healing properties effectively. Therefore, it is expected to prepare a rubber with excellent mechanical and self-healing properties simultaneously by introducing the coordination interactions to form the metal-ligand crosslinking networks, which have the highest bond energy among the non-covalent interactions. Based on the above-mentioned, commercial nitrile–butadiene rubber (NBR) seems to be an ideal choice for rubber with self-healing and recyclable properties. The cyano groups in NBR could react with various transition metal ions to form a metal-ligand crosslinking network effectively [23, 24]. The dynamic reversible behavior in the metal-ligand crosslinking networks can endow rubber with the self-healing and recyclable features [25].

In this research, a simple strategy was utilized to prepare the self-healing and recyclable NBR. The strategy is based on the formation of a metal-ligand crosslinking network between the cyano group and metal ions. With the reversible dynamic crosslinking network, the NBR vulcanizate with excellent self-healing and recyclable properties could be achieved successfully.

2. Experimental

2.1. Materials

Nitrile–butadiene rubber (NBR, 4155 type, 41 wt% acrylonitrile content and ML_{1+4}[100 °C] = 55±5) was used in present research and obtained from Nantex Industry Co. Ltd. (Zhenjiang, China). Cupric sulfate anhydrous ($CuSO_4$, AR) was procured from Reagent Chemical Co. Ltd. (Tianjin, China). Dioctyl phthalate (DOP) plasticizer was sourced from Guangcheng Chemical Industry Co. Ltd. (Tianjin, China).

2.2. Sample preparation

The NBR was initially mixed with DOP in a two-roll mill (X[S] K-160, Qun Yi Rubber Machinery Co. Ltd., Shanghai, China) for 5 min at room temperature. Subsequently, $CuSO_4$ powder was introduced into NBR and the blending process proceeded for another 5 min to ensure the uniform dispersion of DOP and $CuSO_4$ particles in the NBR matrix. The resulting mixture was subjected to compression molding at 180 °C for 60 min using a plate vulcanizing machine (50 T, Qun Yi Rubber Machinery Co. Ltd., Shanghai, China) and the series NBR/$CuSO_4$/DOP vulcanizates with coordination crosslinking induced by metal-ligand interactions was prepared. The above NBR vulcanizates were formed into 2 mm thick sheets.

For the convenience of narration, the vulcanizates were designated according to their NBR/$CuSO_4$/DOP composition. For instance, NCu10-D10 was used to refer to the NBR/$CuSO_4$/DOP (100/10/10) vulcanizate. The specific compositions of the NBR/$CuSO_4$/DOP vulcanizates are summarized in Table 1. For illustrating purposes, the unvulcanized NCu10-D10 blend was noted as NCu10-D10a and the vulcanized NCu10-D10 vulcanizate was noted as NCu10-D10b.

2.3. Characterization

The curing behavior of the NBR/$CuSO_4$/DOP vulcanizates was investigated using a Rotorless Rheometer (KY-6002, Kai Yuan Machinery Co. Ltd., China)

Table 1. Ingredients [phr] of NBR/$CuSO_4$/DOP vulcanizates.

Sample	NCu3-D10	NCu5-D10	NCu10-D10	NCu20-D10
NBR	100	10	100	100
$CuSO_4$	3	5	10	20
DOP	10	10	10	10

at a constant temperature of 180 °C and a vibrating angle of ±1°.

The glass transition temperature (T_g) of the samples was investigated using a differential scanning calorimeter (DSC 204 F1, NETZSCH Instruments, Germany) under a nitrogen atmosphere. The samples were heated at a rate of 10 K/min from –60 to 70 °C to determine their T_g values.

X-ray photoelectron spectra (XPS) survey scans were analyzed by an EscalabTM 250Xi X-ray photoelectron spectrometer (Thermo Fisher Scientific, USA). The chemical components related to nitrogen in NBR/$CuSO_4$/DOP vulcanizates were analyzed to examine their chemical species.

The mechanical properties of NBR/$CuSO_4$/DOP vulcanizates were evaluated using a universal material testing machine (TCS-2000, GoTech Testing Machines Inc., China) at room temperature, with a crosshead speed of 500 mm·min^{-1}. Each sample was tested a minimum of three times to ensure precision and reproducibility.

For the self-healing test, an original dumbbell-shaped sample was cut into two separate pieces using a clean razor blade. The cutting surfaces were aligned and adjoined immediately with minimal pressure. Subsequently, the healed samples were subjected to the healing treatment at the predetermined temperature for a certain time without loading. After healing, the mechanical properties were assessed through stress-strain testing. The healing efficiency was calculated as the ratio of the tensile strength of the healed sample to that of the original one.

The morphology of NBR/$CuSO_4$/DOP vulcanizates was investigated by the utilization of field-emission scanning electron microscopy (FE-SEM, JSM-6700F, Japan Electron Optics Laboratory Co., Ltd., Japan). Prior to analysis, the surfaces of the samples were sputter-coated with a thin layer of platinum coating to prevent electrostatic accumulation.

Tensile stress relaxation experiments were conducted using a high-temperature and low-temperature servo-controlled tensile testing machine (AI-7000S, GoTech Testing Machines Inc., China) at room temperature (*RT*), 60, 120 and 180 °C, respectively. The sample were subjected to a strain of 100% at a constant crosshead speed of 100 mm·min^{-1}. The sample were tested after a 5 min incubation period, and the relaxation time was set at 5 min.

Equilibrium swelling experiments were conducted to ascertain the crosslinking density of the NBR/$CuSO_4$/DOP vulcanizates. Initially, the samples were submerged in dichloromethane (DCM) for a period of 7 days to attain the swelling equilibrium. Then the surface of the swollen samples was gently blotted using the dust-free filter paper to remove any residual DCM, and the samples were subsequently weighed. Finally, the swollen samples were dried at 60 °C for a duration of 12 hours until a constant weight was achieved. The crosslinking density of samples was computed by the Flory-Rehner equation as shown as Equation (1) [26]:

$$V = -\frac{\ln(1-V_0) + V_0 + \chi V_0^2}{V_1\left(V_0^{1/3} - \frac{V_0}{2}\right)} \quad (1)$$

where V_0 is given by Equation (2):

$$V_0 = \frac{\frac{m_2}{\rho_2}}{\frac{m_2}{\rho_2} + \frac{m_1 - m_2}{\rho_1}} \quad (2)$$

The crosslinking density (V) of the samples was calculated using the formula above, where V_1 represented the molar volume of dichloromethane (DCM) at 67.8 cm^3·mol^{-1}, χ was the NBR-DCM interaction parameter at 0.33, ρ_1 and ρ_2 were the densities of DCM and NBR at 1.325 and 0.98 g·cm^{-3}, respectively. The mass of the swollen sample before and after drying was represented as m_1 and m_2, respectively.

3. Results and discussion

3.1. Curing characteristics and coordination crosslinking behaviors of NBR/$CuSO_4$/DOP vulcanizates

In our research, a distinctive characteristic of self-healing rubber is the formation of a coordination crosslinking network through the reversible coordination bonds, which is achieved by utilizing the metal-ligand interaction of cyano in NBR with $CuSO_4$. A schematic illustration of this process is presented in Figure 1. Our previous work has demonstrated that the unmodified commercial NBR can engage in coordination interactions with metal salts to establish a stable coordination crosslinking network [27]. This strategy ensures the formation of supramolecular networks in NBR/$CuSO_4$/DOP compounds based on dynamic bonds.

Under the stimulation of heat treatment, the cyano group in NBR will react with the copper ion in $CuSO_4$ by coordination effectively. During the vulcanization, the chain mobility of the NBR is decreased obviously due to the implication of metal-ligand interactions, which can be derived from the analysis of

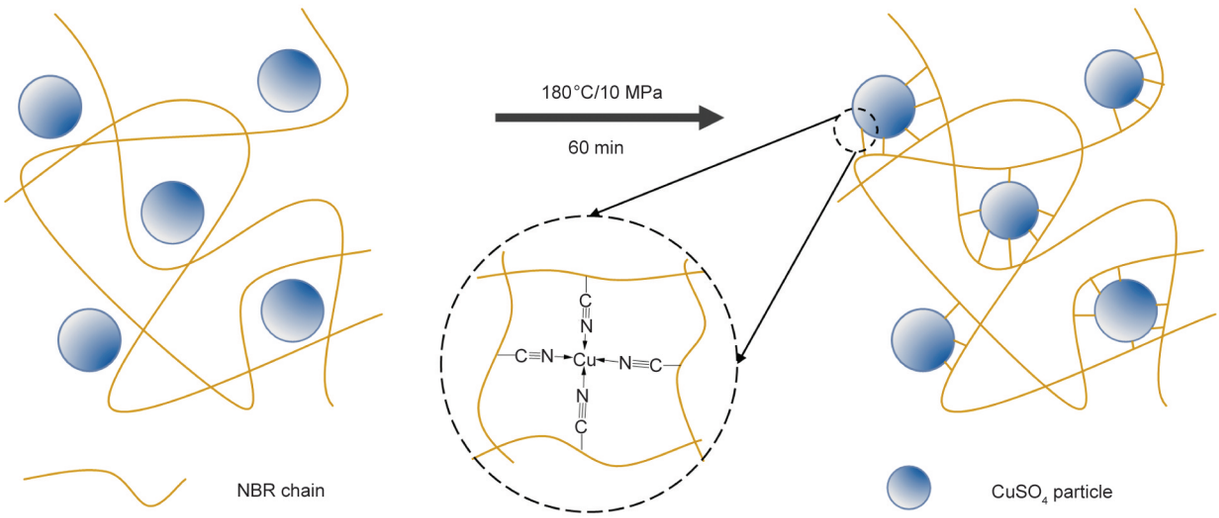

Figure 1. Diagrammatical illustration of the coordination crosslinking structure in NBR vulcanizate.

curing curves as shown in Figure 2. As seen in the figure, the series NBR/$CuSO_4$/ DOP compounds with different $CuSO_4$ dosages at 180 °C. The torque of the compounds was increased with increasing curing time, resulting from the formation of the coordination crosslinking networks induced by the interaction between the cyano group and Cu^{2+}. Moreover, the torque was also increased with increasing $CuSO_4$ dosage, which could attribute to the increasing crosslinking density.

The glass transition temperature (T_g) is a useful indicator of the mobility of macromolecular segments. Comparing the T_g values of the NBR/$CuSO_4$/DOP blend with that of the vulcanizates, it is possible to identify the occurrence of crosslinking within the NBR/$CuSO_4$/DOP vulcanizates. The T_g of the series NBR/$CuSO_4$/DOP blend and the vulcanizates were measured by DSC. The DSC curves are displayed in Figure 3. It is evident that the T_g of the series of the pure NBR and NBR/$CuSO_4$/DOP blend did not show significant changes in T_g of the series (–22.1 and –21.6 °C), indicating that the simple blending of $CuSO_4$ with NBR did not result in the considerable crosslinking between Cu^{2+} and a cyano group. However, after vulcanization, the T_g of the series value of NCu10-D10 increased significantly from –21.6 to –15.1 °C, indicating the formation of a coordination crosslinking network through the strong coordination effect of Cu^{2+} and cyano group. The crosslinking network greatly restricted the mobility of NBR chain segments greatly, resulting in significantly increasing T_g of the series values. Moreover, the T_g of the series values of the NBR/$CuSO_4$/DOP vulcanizates were increased with the increasing $CuSO_4$ dosage, indicating that the higher the $CuSO_4$ content led to the higher the crosslinking density, which

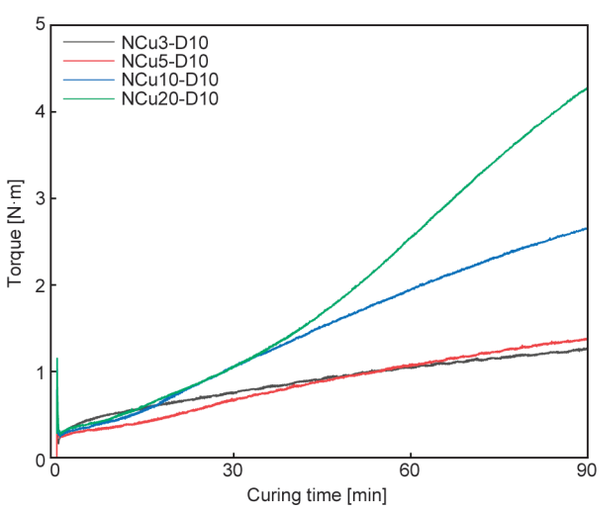

Figure 2. Curing curves of NBR/$CuSO_4$/DOP compounds with different $CuSO_4$ dosage at 180 °C.

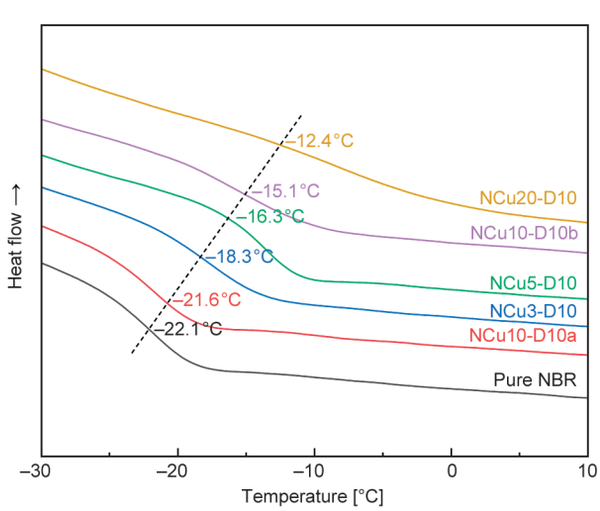

Figure 3. DSC curves of NBR/$CuSO_4$/DOP blend and vulcanizates.

resulted in the strongly restricted movement of NBR chain segments.

XPS could identify the chemical environments of elements by detecting their characteristic binding energies. Coordination structures, such as those formed between metal ions and ligands, can significantly alter the chemical environment of the central and ligand atoms. In this research, the N 1s XPS spectra of NBR/$CuSO_4$/DOP blend and vulcanizates were analyzed to investigate the occurrence of coordination reactions. As illustrated in Figure 4a, the N 1s spectra of the NBR/$CuSO_4$/DOP blend reveal a solitary nitrogen environment, displaying a central binding energy of 399.3 eV, which belonged to the nitrogen atoms of free cyano groups. However, after vulcanization, as illustrated in Figure 4b, a new peak appeared at higher binding energy (401.6 eV), and the shift is caused by the coordination of the cyano group with Cu^{2+}, which results in a transfer of electrons from the nitrogen atom to the metal ions [28]. The resulting increase in the internal electron binding energy of the coordinated nitrogen atoms leads to a different chemical environment compared to that of the NBR/$CuSO_4$/DOP blend without coordination, resulting in a shoulder peak at the higher binding energy in the XPS spectrum. These observations provide supporting evidence for forming coordination structures between Cu^{2+} and cyano groups in the NBR/$CuSO_4$/DOP vulcanizates.

3.2. Mechanical properties of NBR/$CuSO_4$/DOP vulcanizates

The stress-strain curves of NBR/$CuSO_4$/DOP vulcanizates with different $CuSO_4$ dosage were shown in Figure 5. The tensile strength of the series vulcanizates was substantially increased with the increasing $CuSO_4$ dosage, while the elongation at break was decreased gradually. For the coordination crosslinking vulcanizates, the metal-ligand coordination bond acts as a 'sacrificial bond', which could improve the tensile strength significantly while can maintain the relative high elongation at break [29, 30]. The increasing $CuSO_4$ dosage improved the coordination efficiency of the cyano group with Cu^{2+} greatly, resulting in an increased crosslinking density of the NBR vulcanizates (as shown in Table 3). Under the external force, the dumbbell-shaped sample was stretched to fracture and more coordination bonds were required to be broken, resulting in increased tensile strength. The mechanical properties of the series NBR/$CuSO_4$/DOP vulcanizates are summarized in Table 2. It can be observed that the tearing strength

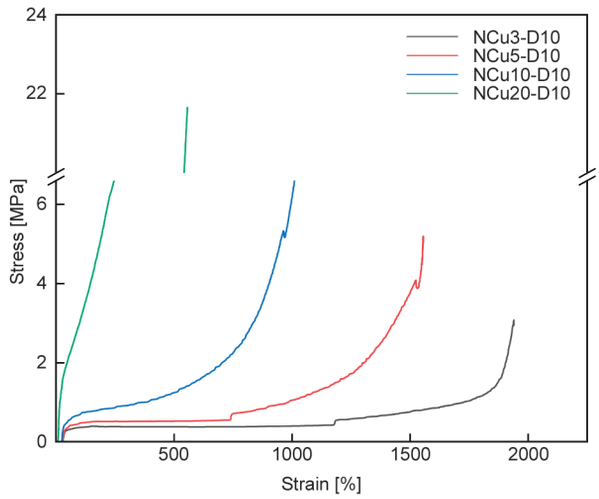

Figure 5. Stress–strain curves of NBR/$CuSO_4$/DOP vulcanizates with different $CuSO_4$ dosage at 180 °C.

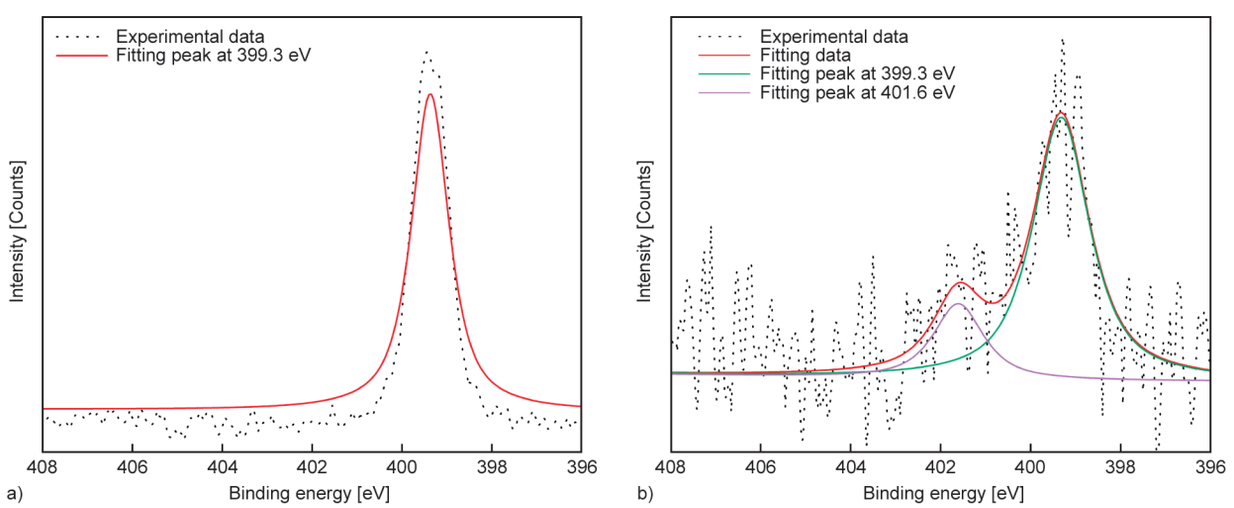

Figure 4. N 1s XPS spectra of NBR/$CuSO_4$/DOP blend and vulcanizate: a) NCu10-D10a; b) NCu10-D10b.

Table 2. Mechanical properties of NBR/$CuSO_4$/DOP vulcanizates.

Samples	Tensile strength [MPa]	Elongation at break [%]	Tearing strength [kN·m^{-1}]	Shore A hardness
NCu3-D10	3.08	1940	8.87	35
NCu5-D10	5.19	1557	10.84	42
NCu10-D10	6.62	1012	18.37	65
NCu20-D10	21.65	578	32.58	78

and Shore A hardness of the vulcanizates were increased with increasing $CuSO_4$ dosage, which can be attributed to the increasing crosslinking density.

3.3. Self-healing properties of NBR/$CuSO_4$/DOP vulcanizates

In order to assess the self-healing ability, the original dumbbell-shaped sample was cut into two separate pieces and then gently rejoined together to ensure good contact between the cutting surfaces, as shown in Figure 6. The samples were then subjected to various temperatures and duration for healing. Subsequently, the stress-strain behavior of the healed samples was tested at a stretch rate of 500 mm·min^{-1} after cooling to room temperature.

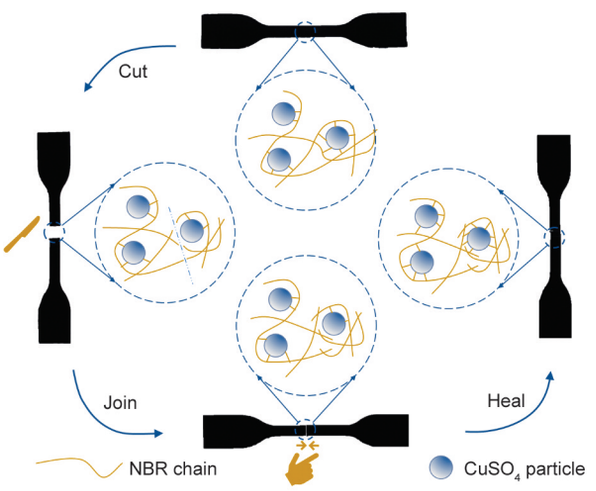

Figure 6. Diagrammatical illustration of self-healing behavior of vulcanizates.

Figure 7 shows the FE-SEM photographs of the cut position of the NCu10-D10 sample before and after healing (180 °C, 60 min). Figure 7a shows the surface of the sample with evident cutting marks, which have clear, sharp edges and an obvious 'step'-like fracture, indicating that the separating cut sample only keeps in contact with each other rather than producing a strong bonding. After healing at 180 °C for 60 min, as shown in Figure 7b, the cutting marks on the sample surface became blurry, and the edges of the cuts fused with each other, and the 'step'-like fractures was disappeared. Only a superficial depression could be found in the cut position, indicating the fine fracture healing after heat treatment.

The healed Dumbbell-shaped sample (180 °C for 60 min) could successfully sustain a 500 g load without breaking, as shown in Figure 8a, indicating the excellent self-healing capability of the NBR vulcanizate. Figure 8b displays the stress-strain curves of NCu10-D10 tested before and after healing at 180 °C for 60 min. It is evident that the healed sample was fractured at 6.4 MPa (the original sample was 6.6 MPa) with a healing efficiency of about 97%. At the elevated temperature, the chain mobility of the vulcanizates can be enhanced obviously, and the NBR molecular chains diffuse each other in the cutting surface. The Cu^{2+} exposed due to bond breakage and the uncoordinated Cu^{2+}, dispersed in NBR could

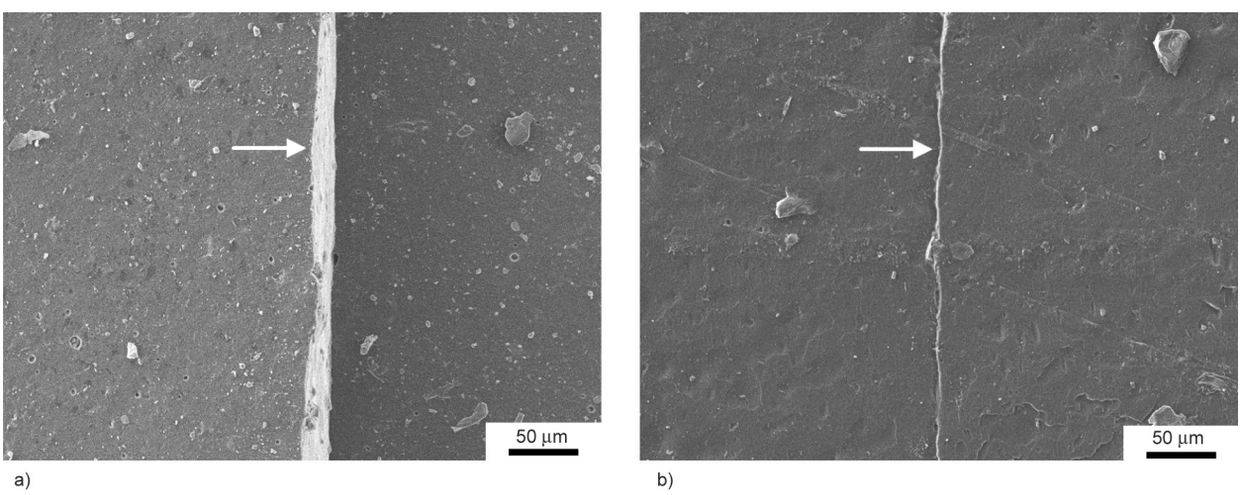

Figure 7. FE-SEM photographs of the cut position of NCu10-D10 before and after healing (180 °C, 60 min): a) before healing; b) after healing.

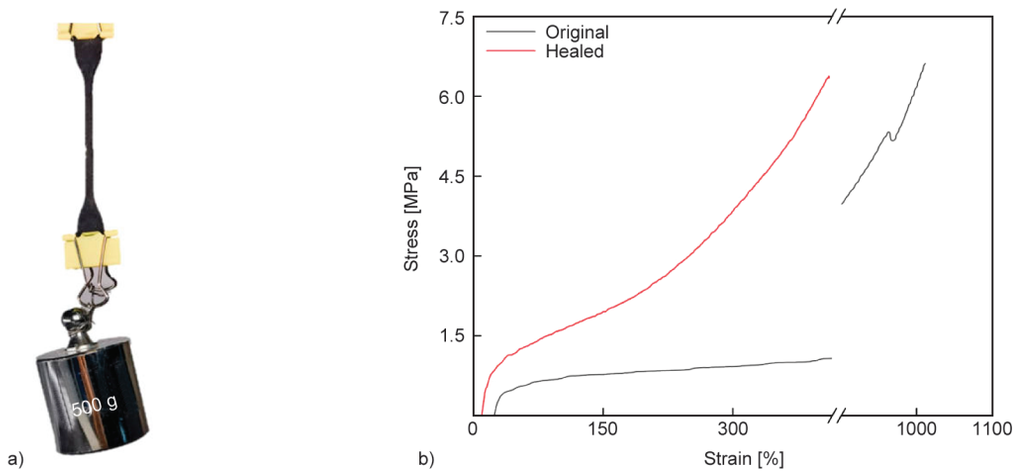

Figure 8. a) Photograph of NCu10-D10 hanging a 500 g load after healing; b) stress-strain curves of NCu10-D10 healed at 180 °C for 60 min.

reorganize with the cyano group to form a well-established network in the cutting surfaces. Moreover, the elastic modulus (as observed from the slope of the stress-strain curves) of the healed NCu10-D10 sample was significantly increased, and the elongation at break was significantly decreased compared to that of the original sample. This can be attributed to the repair of broken coordination bonds in the cutting surface and the formation of new coordination bonds during the healing treatment, resulting in increased crosslinking density. It is notable that, during the testing of the tensile strength of healed samples, many samples were not fractured at the cut position (refer to Figure 9), which is valuable evidence of the vulcanizate's excellent self-healing ability.

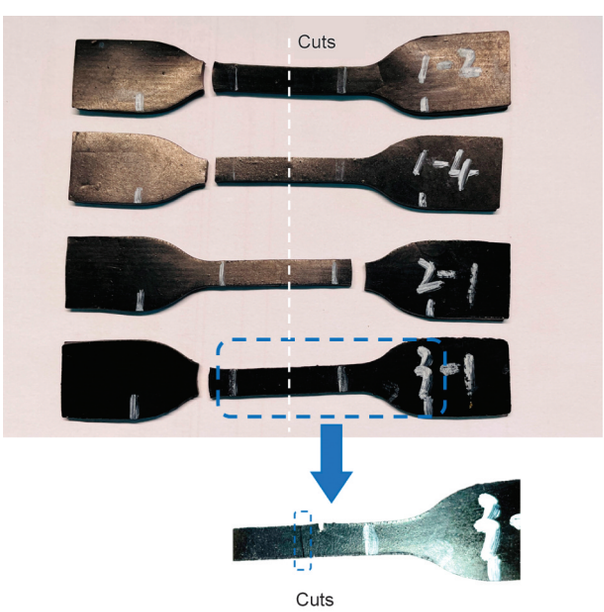

Figure 9. Digital photograph of the healed sample after fracture (Sample incisions are marked with white dashed lines).

Figure 10a illustrates the tensile strength of NCu10-D10 sample healed at different healing temperatures for different times. As can be seen from Figure 10a, the tensile strength of vulcanizates after healing was increased with the healing temperature and healing time remarkably. Under the same healing temperature and healing time (1 h, 60 °C), our study demonstrates higher tensile strength and healing efficiency than Mandal *et al.*'s work in 2021 [31]. Usually, the self-healing ability of the coordination bond-based materials is influenced by the viscosity of the interface, the diffusive mobility of molecular chain segments and the exchanging rate of coordination bonds [32, 33]. The coordination bond-based self-healing process involves both the reorganization and exchange of coordination bonds and the faster exchange rate of coordination bonds could improve the self-healing efficiency. Increasing the healing temperature and time can remarkably accelerate the diffusion rate of molecular chains and the exchange rate of coordination bonds.

Reorganization of the coordination crosslinked network is an important mechanism underlying the self-healing behavior of vulcanizates. To further investigate the reorganization of the coordination crosslinking network, the tensile stress relaxation experiments were conducted at various temperatures, as shown in Figure 10b. Generally, the stress relaxation curves of NBR vulcanizate exhibit a continuous decrease of stress with increasing relaxation time and the higher temperature could accelerate the stress relaxation. However, it was surprising to find that the stress relaxation curves of NCu10-D10 sample exhibited an abnormal phenomenon. With increasing temperature, the stress relaxation rate of NCu10-D10

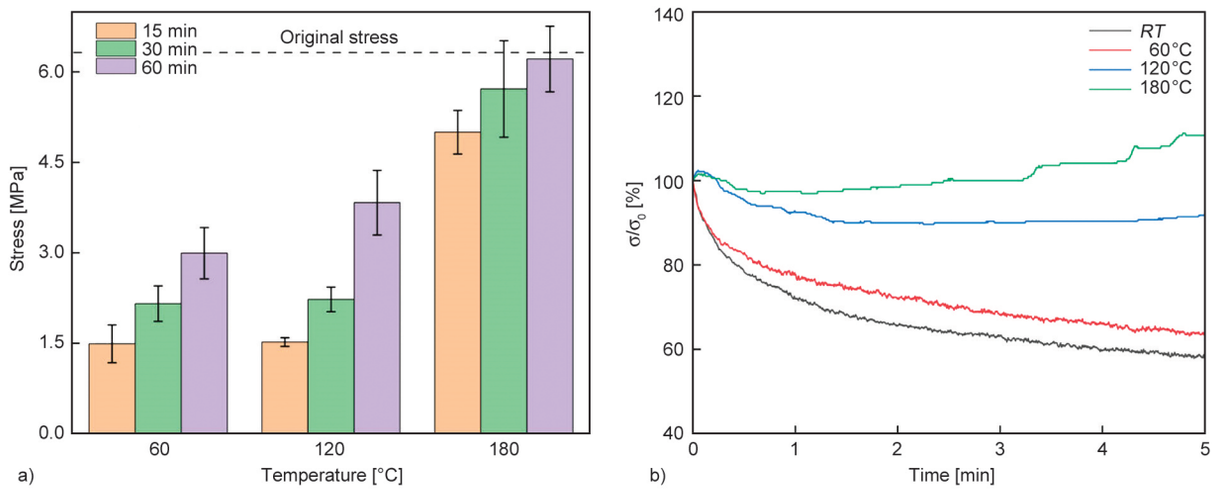

Figure 10. a) Tensile strength of NCu10-D10 healed at different temperature and time; b) tensile stress relaxation curves of NCu10-D10 at different temperature with 100% strain.

was significantly decreased. Interestingly, the stress relaxation curves of NCu10-D10 even exhibited stress recovery at 120 and 180 °C. This can be attributed to the reorganization of the coordination crosslinked network in the NBR vulcanizate under high temperature. The elevation of temperature accelerated the rate of coordination bond exchange, strengthening the coordination crosslinked network of the vulcanizate and requiring great force to maintain the original strain. Increasing healing temperature, the reorganization of the coordination crosslinked network in the vulcanizate occurred more rapidly, which was consistent with the influence of temperature on the healing strength, as shown in Figure 10a.

It should be noted that the influence of increasing healing temperature on the healing efficiency of the NBR vulcanizate is more sensitive than that of increasing healing time, as shown in Figure 11 and Figure 10a. Notably, the healing efficiency of the vulcanizates was only 16.7% after 72 h healing at room temperature, indicating that the coordination crosslinking network of vulcanizates is not active at room temperature. The lower temperature limits the exchange rate of coordination bonds, which hinders them from rebuilding in the short term after breaking. It also implies that the coordination crosslinking network is reversible, which could enable the recycling of vulcanizates through appropriate methods.

3.4. Recycling properties of NBR/CuSO$_4$/DOP vulcanizates

The recycled method of vulcanizates is shown in Figure 12. NCu10-D10 scraps were sheared using a two-roll mill for 20 min to obtain the plasticity, then

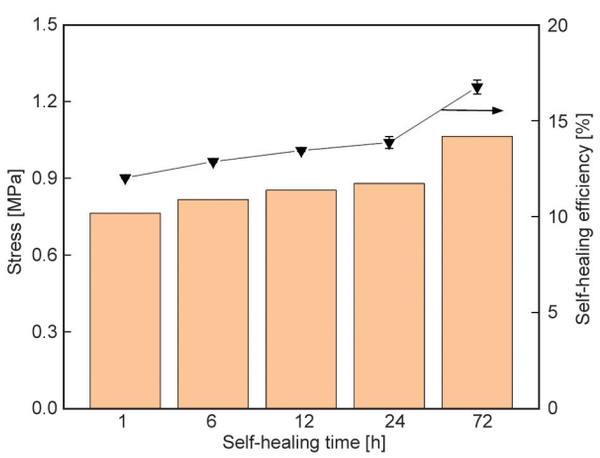

Figure 11. Tensile strength and healing efficiency of NCu10-D10 healed at different times at room temperature.

followed by hot-pressing at 180 °C for 20 min using a plate vulcanizing machine. The surface of the recycled vulcanizate was smooth and flat. Moreover, compared with the original vulcanizate, there was no discernible difference in appearance in the recycled vulcanizate.

We conducted serial tests to verify the recycling effect of vulcanizates after the mechanical shear.

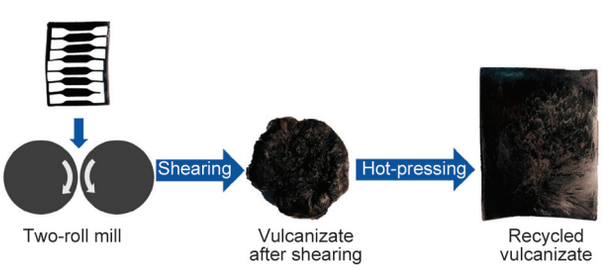

Figure 12. Schematic diagram of recycling method of vulcanizates.

Figures 13a, and 13b displays the N 1s XPS spectra of NCu10-D10 after being subjected to mechanical shearing and re-vulcanization. The N 1s spectra of NCu10-D10 after mechanical shearing exhibited a singular nitrogen environment with a central binding energy of 399.3 eV. This value is consistent with the N 1s spectra of the NBR/$CuSO_4$/DOP blend, which is shown in Figure 4a. It indicates that the coordination crosslinking network of vulcanizates underwent a reversible transformation after mechanical shearing and reverted to the unvulcanized condition. However, a shoulder peak appeared at a higher binding energy after the re-vulcanization, indicating that the re-vulcanized vulcanizates could recover the coordination structure after hot-pressing. Figure 13c shows the DSC curves of NCu10-D10 before and after mechanical shearing and re-vulcanized. Similarly, the transition of T_g in NCu10-D10 before and after mechanical shearing and the re-vulcanized process is attributed to the reversible transformation of the coordination crosslinking network. The coordination bonds in vulcanizates are broken by the strong mechanical shear force, reducing the constraint of the NBR chain segments and reducing the T_g value. After re-vulcanization, the coordination crosslinking network of vulcanizates is reconstructed with a subsequent increase in T_g. The T_g of the re-vulcanized vulcanizates is higher than that of the NBR vulcanizates, which should be due to the higher crosslinking density (refer to Table 3). Figure 13d shows the stress-strain curves of NCu10-D10 after the re-vulcanization treatment. The tensile strength of the re-vulcanized vulcanizate was almost the same compared to the original sample. Moreover, an increase in elastic modulus (as observed from the slope of the stress-strain curves) of re-vulcanized NCu10-D10

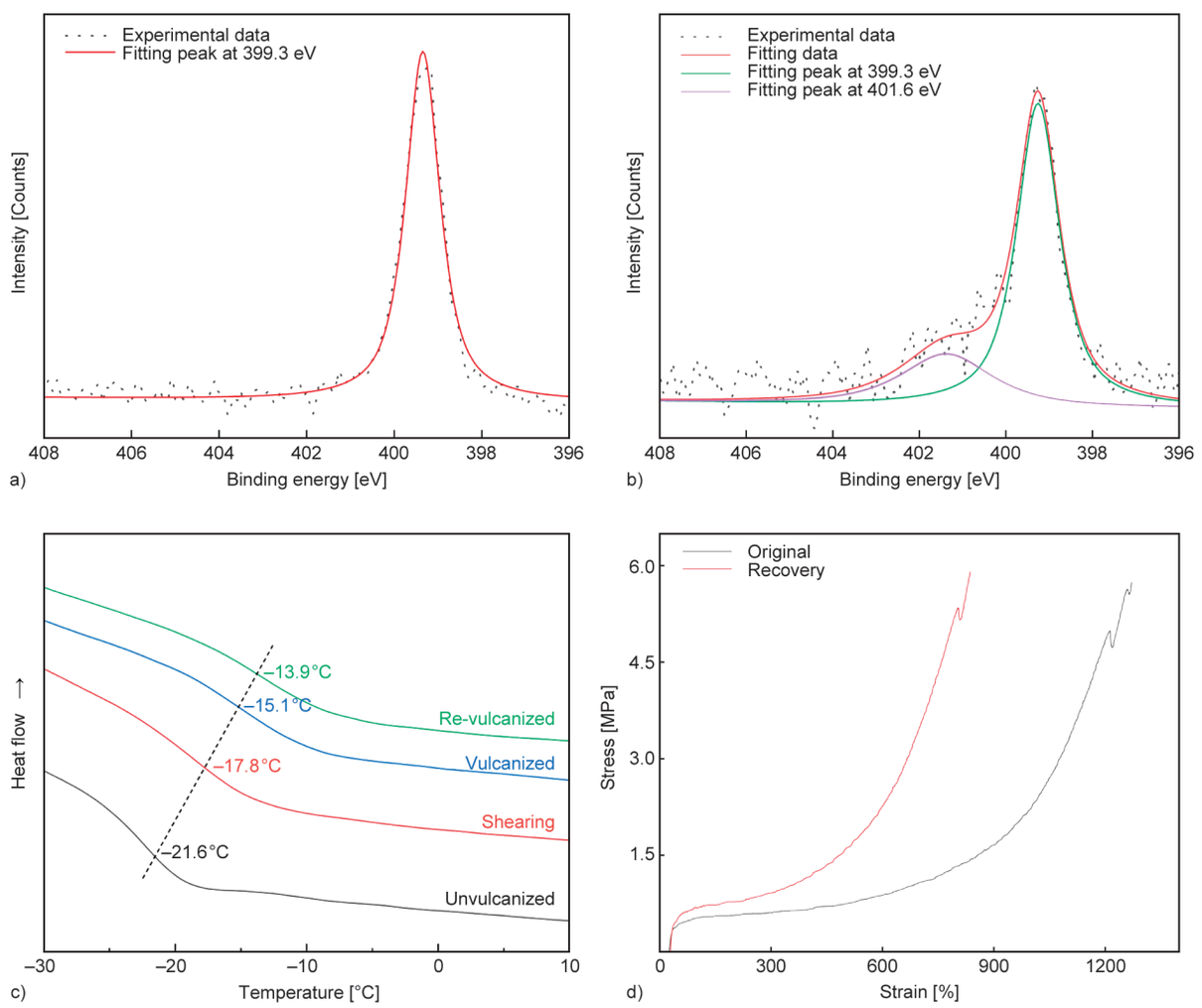

Figure 13. a) N 1s XPS spectra of NCu10-D10 after shearing and b) re-vulcanized; c) DSC curves of NCu10-D10 with recycled process; d) stress-strain curves of NCu10-D10 after re-vulcanization.

was also observed in Figure 13d, which can be attributed to the increased crosslinking density of the re-vulcanized NBR vulcanizate.

3.5. Swelling properties of NBR/$CuSO_4$/DOP vulcanizates

The coordination crosslinking behavior of the series NCu10-D10 vulcanizates was visually investigated by the swelling experiments, as shown in Figure 14. The unvulcanized NCu10-D10 was completely dissolved by DCM at room temperature, indicating that the NBR matrix was not crosslinked. Interestingly, the mechanical sheared NCu10-D10 sample was almost completely dissolved after 24 h of immersion in DCM as well, indicating that the coordination crosslinking network had already disappeared after mechanical shear. Conversely, the vulcanized NCu10-D10 and re-vulcanized NCu10-D10 could not be dissolved completely but only partially swelled, indicating that the crosslinking between the cyano group and Cu^{2+} had occurred after hot-pressing. After 24 hours of immersion, the re-vulcanized NCu10-D10 exhibited less swelling compared to the vulcanized NCu10-D10, indicating the formation of more crosslinking points between molecular chain segments in the re-vulcanized NCu10-D10. The observation agrees with the crosslinking density calculated using the Flory-Rehner equation, as shown in Table 3.

Table 3. Dissolvability and crosslinking density of NBR/$CuSO_4$/DOP blend and vulcanizates by swelling at equilibrium.

Sample	Dissolvability	Crosslinking density $\cdot 10^{-5}$ [mol/cm^3]
NCu3-D10	×	0.13
NCu5-D10	×	0.37
NCu10-D10a	√	/
NCu10-D10b	×	2.11
Sheared NCu10-D10	√	/
Re-vulcanized NCu10-D10	×	2.79
NCu20-D10	×	3.45

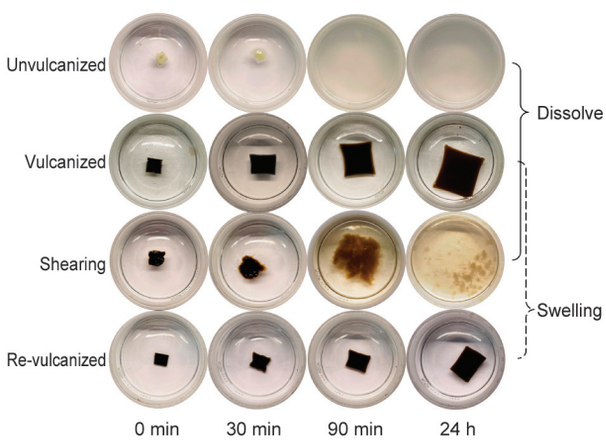

Figure 14. Digital pictures of swelling experiments in DCM of series NCu10-D10 vulcanizates.

4. Conclusions

In conclusion, a facile strategy was developed to create an NBR with remarkable mechanical properties, excellent self-healing, and recycling abilities by introducing metal-ligand coordination interactions through simple mechanical blending. The curing curves, DSC, XPS, and equilibrium swelling experiments demonstrated the successful formation of the coordination crosslinking network. Crosslinking of NBR chains was achieved by using Cu^{2+}-cyano coordination bonds instead of conventional crosslinking agents such as sulfur or peroxide. The $CuSO_4$ dosage strongly affects the mechanical properties of the prepared vulcanizates, and the vulcanizates exhibited excellent mechanical properties, including a stretchability of up to 1900% (NCu3-D10) and a tensile strength of up to 21.7 MPa (NCu20-D10). Moreover, the NBR/$CuSO_4$/DOP vulcanizates possessed the excellent self-healing and recycling properties, which is due to the dynamic reversibility of the coordination crosslinking network. The healing temperature and healing time played a critical role in determining the self-healing properties of the vulcanizates, with a remarkable healing efficiency of up to 97% of the original tensile strength achieved after healing at 180 °C for 60 min. Furthermore, the tensile strength of the NBR/$CuSO_4$/DOP vulcanizates after recycling was comparable to that of the original sample. It is believed that this strategy of preparing a combination of excellent mechanical and self-healing properties has great potential for application in other polar polymers.

Acknowledgements

The work was supported by the Shandong Provincial Natural Science Foundation, China [grant number ZR2021ME028].

References

[1] White S. R., Sottos N. R., Geubelle P. H., Moore J. S., Kessler M. R., Sriram S., Brown E. N., Viswanathan S.: Autonomic healing of polymer composites. Nature, **409**, 794–797 (2001). https://doi.org/10.1038/35057232

[2] Habault D., Zhang H., Zhao Y.: Light-triggered self-healing and shape-memory polymers. Chemical Society Reviews, **42**, 7244–7256 (2013). https://doi.org/10.1039/C3CS35489J

[3] Das A., Sallat A., Böhme F., Suckow M., Basu D., Wießner S., Stöckelhuber K. W., Voit B., Heinrich G.: Ionic modification turns commercial rubber into a self-healing material. ACS Applied Materials and Interfaces, **7**, 20623–20630 (2015). https://doi.org/10.1021/acsami.5b05041

[4] Xu C., Cao L., Lin B., Liang X., Chen Y.: Design of self-healing supramolecular rubbers by introducing ionic cross-links into natural rubber *via* a controlled vulcanization. ACS Applied Materials and Interfaces, **8**, 17728–17737 (2016). https://doi.org/10.1021/acsami.6b05941

[5] Ryu Y. S., Oh K. W., Kim S. H.: Synthesis and characterization of a furan-based self-healing polymer. Macromolecular Research, **24**, 874–880 (2016). https://doi.org/10.1007/s13233-016-4122-5

[6] Hou H. H., Yin J., Jiang X. S.: Reversible diels-alder reaction to control wrinkle patterns: From dynamic chemistry to dynamic patterns. Advanced Materials, **28**, 9126–9132 (2016). https://doi.org/10.1002/adma.201602105

[7] Lai Y., Kuang X., Zhu P., Huang M. M., Dong X., Wang D. J.: Colorless, transparent, robust, and fast scratch-self-healing elastomers *via* a phase-locked dynamic bonds design. Advanced Materials, **30**, 1802556 (2018). https://doi.org/10.1002/adma.201802556

[8] Cordier P., Tournilhac F., Soulie-Ziakovic C., Leibler L.: Self-healing and thermoreversible rubber from supramolecular assembly. Nature, **451**, 977–980 (2008). https://doi.org/10.1038/nature06669

[9] Xu C., Cao L., Huang X., Chen Y., Lin B., Fu L.: Self-healing natural rubber with tailorable mechanical properties based on ionic supramolecular hybrid network. ACS Applied Materials and Interfaces, **9**, 29363–29373 (2017). https://doi.org/10.1021/acsami.7b09997

[10] Wang Z., Xie C., Yu C., Fei G., Wang Z., Xia H.: A facile strategy for self-healing polyurethanes containing multiple metal-ligand bonds. Macromolecular Rapid Communications, **39**, 1700678 (2018). https://doi.org/10.1002/marc.201700678

[11] Cui X., Song Y., Wang J-P., Wang J-K., Zhou Q., Qi T., Li G. L.: Self-healing polymers with tunable mechanical strengths *via* combined hydrogen bonding and zinc-imidazole interactions. Polymer, **174**, 143–149 (2019). https://doi.org/10.1016/j.polymer.2019.04.060

[12] Kasem H., Shriki H., Ganon L., Mizrahi M., Abd-Rbo K., Domb A. J.: Rubber plunger surface texturing for friction reduction in medical syringes. Friction, **7**, 351–358 (2019). https://doi.org/10.1007/s40544-018-0227-5

[13] Ramezani M., Ripin Z. M., Ahmad R.: Computer aided modelling of friction in rubber-pad forming process. Journal of Materials Processing Technology, **209**, 4925–4934 (2009). https://doi.org/10.1016/j.jmatprotec.2009.01.015

[14] Jaafar C. N. A., Zainol I., Ishak N. S., Ilyas R. A., Sapuan S. M.: Effects of the liquid natural rubber (LNR) on mechanical properties and microstructure of epoxy/silica/kenaf hybrid composite for potential automotive applications. Journal of Materials Research and Technology, **12**, 1026–1038 (2021). https://doi.org/10.1016/j.jmrt.2021.03.020

[15] Rodriguez N., Dorogin L., Chew K. T., Persson B. N. J.: Adhesion, friction and viscoelastic properties for non-aged and aged styrene butadiene rubber. Tribology International, **121**, 78–83 (2018). https://doi.org/10.1016/j.triboint.2018.01.037

[16] Li B., Li S-X., Shen M-X., Xiao Y-L., Zhang J., Xiong G-Y., Zhang Z-N.: Tribological behaviour of acrylonitrile-butadiene rubber under thermal oxidation ageing. Polymer Testing, **93**, 106954 (2021). https://doi.org/10.1016/j.polymertesting.2020.106954

[17] Asaro L., Gratton M., Seghar S., Hocine N. A.: Recycling of rubber wastes by devulcanization. Resources, Conservation and Recycling, **133**, 250–262 (2018). https://doi.org/10.1016/j.resconrec.2018.02.016

[18] Molanorouzi M., Mohaved S. O.: Reclaiming waste tire rubber by an irradiation technique. Polymer Degradation and Stability, **128**, 115–125 (2016). https://doi.org/10.1016/j.polymdegradstab.2016.03.009

[19] Movahed S. O., Ansarifar A., Zohuri G., Ghaneie N., Kermany Y.: Devulcanization of ethylene–propylene–diene waste rubber by microwaves and chemical agents. Journal of Elastomers & Plastics, **48**, 122–144 (2016). https://doi.org/10.1177/0095244314557975

[20] Shields Y., De Belie N., Jefferson A., van Tittelboom K.: A review of vascular networks for self-healing applications. Smart Materials and Structures, **30**, 063001 (2021). https://doi.org/10.1088/1361-665X/abf41d

[21] Peng T., Huang J., Gong Z., Chen X., Chen Y.: Self-healing of reversibly cross-linked thermoplastic vulcanizates. Materials Chemistry and Physics, **292**, 126804 (2022). https://doi.org/10.1016/j.matchemphys.2022.126804

[22] Liu Y., Li Z., Liu R., Liang Z., Yang J., Zhang R., Zhou Z., Nie Y.: Design of self-healing rubber by introducing ionic interaction to construct a network composed of ionic and covalent cross-linking. Industrial and Engineering Chemistry Research, **58**, 14848–14858 (2019). https://doi.org/10.1021/acs.iecr.9b02972

[23] Shen F., Yuan X-F., Guo W-H., Wu C-F.: Coordination crosslinking of nitrile rubber filled with copper sulfate particles. Chinese Journal of Polymer Science, **25**, 447–459 (2007). https://doi.org/10.1142/S0256767907002345

[24] Mou H., Shen F., Shi Q., Liu Y., Wu C., Guo W.: A novel nitrile butadiene rubber/zinc chloride composite: Coordination reaction and miscibility. European Polymer Journal, **48**, 857–865 (2012).
https://doi.org/10.1016/j.eurpolymj.2012.02.004

[25] Li C-H., Zuo J-L.: Self-healing polymers based on coordination bonds. Advanced Materials, **32**, 1903762 (2020).
https://doi.org/10.1002/adma.201903762

[26] Flory P. J.: Statistical mechanics of swelling of network structures. The Journal of Chemical Physics, **18**, 108–111 (1950).
https://doi.org/10.1063/1.1747424

[27] Sun Y., Wang J., Sun L., Hua J., Wang Z.: Synergistic effect of copper sulfate and tetramethylthiuram monosulfide induced metal-coordination cross-linking in nitrile–butadiene rubber. Macromolecular Materials and Engineering, **306**, 2100057 (2021).
https://doi.org/10.1002/mame.202100057

[28] Cano A., Avila Y., Avila M., Reguera E.: Structural information contained in the XPS spectra of nd^{10} metal cyanides. Journal of Solid State Chemistry, **276**, 339–344 (2019).
https://doi.org/10.1016/j.jssc.2019.05.021

[29] Liu J., Wang S., Tang Z., Huang J., Guo B., Huang G.: Bioinspired engineering of two different types of sacrificial bonds into chemically cross-linked cis-1,4-polyisoprene toward a high-performance elastomer. Macromolecules, **49**, 8593–8604 (2016).
https://doi.org/10.1021/acs.macromol.6b01576

[30] Liu Y., Tang Z., Wu S., Guo B.: Integrating sacrificial bonds into dynamic covalent networks toward mechanically robust and malleable elastomers. ACS Macro Letters, **8**, 193–199 (2019).
https://doi.org/10.1021/acsmacrolett.9b00012

[31] Mandal S., Simon F., Banerjee S. S., Tunnicliffe L. B., Nakason C., Das C., Das M., Naskar K., Wiessner S., Heinrich G., Das A.: Controlled release of metal ion cross-linkers and development of self-healable epoxidized natural rubber. ACS Applied Polymer Materials, **3**, 1190–1202 (2021).
https://doi.org/10.1021/acsapm.1c00039

[32] Bode S., Enke M., Bose R., Schacher F., Garcia S., van der Zwaag S., Hager M., Schubert U.: Correlation between scratch healing and rheological behavior for terpyridine complex based metallopolymers. Journal of Materials Chemistry A, **3**, 22145–22153 (2015).
https://doi.org/10.1039/C5TA05545H

[33] Wang D-P., Lai J-C., Lai H-Y., Mo S-R., Zeng K-Y., Li C-H., Zuo J-L.: Distinct mechanical and self-healing properties in two polydimethylsiloxane coordination polymers with fine-tuned bond strength. Inorganic Chemistry, **57**, 3232–3242 (2018).
https://doi.org/10.1021/acs.inorgchem.7b03260